ORIGINAL PAPER

Investigation of Micropolar Hybrid Nanofluid (Iron Oxide–Molybdenum Disulfide) Flow Across a Sinusoidal Cylinder in Presence of Magnetic Field

Kh. Hosseinzadeh[1] · M. R. Mardani[1] · Sajad Salehi[1] · M. Paikar[1] · D. D. Ganji[1]

Abstract

The purpose of this paper is to investigate the micropolar nanofluid flow across a sinusoidal cylinder in presence of the magnetic field. The base fluid is an equal mixture of ethylene glycol and water; also,ithybridized by iron oxide (Fe_3O_4) andMolybdenum disulfide (MoS_2) nanoparticles.In this study, equations are transformed from PDEs to ODEs and solved by Rung-Kutta fifth-order. After solving the equations, it can be seen that various nondimension parameters are involved (e.g.micro-polar parameter, nanoparticle volume fraction, shape factor, and magnetic field parameter), therefore a sensitivity analysis is applied to investigate the effect ofinvolvedparameters. Besides, variation of Nusselt number and skin friction coefficient are studied.Further analysis showed that Nusselt number is an increasing function of volume fraction and increment in the magnetic field leads to higherskin friction coefficient.Also, whenmicro-gyrationis zero the microelements in the vicinity of the wall are unable to rotate, and by increasing micro-gyration parameters these microelements meet rotation.As a novelty, the hybrid Micropolar nanofluid suspends in mixture fluid flow in sinusoidal cylinder geometry have been investigated. The magnetic force and rotational velocity have been considered.

Keywords Sinusoidal cylinder · Micropolar nanofluid · Mixture fluid · Magnetic field

List of Symbols

x, y, z	Direction components
U, V, W	Velocity components
α_{nf}	Thermal diffusivity of nanofluid
μ_{nf}	Viscosity of nanofluid
μ_f	Viscosity of fluid
$(C_p)_{nf}$	Heat capacity of nanofluid
k_{nf}	Thermal conductivity of nanofluid

✉ Kh. Hosseinzadeh
Khashayar_h68@yahoo.com

[1] Department of Mechanical Engineering, Babol Noshirvani University of Technology, Babol, Iran

k_f	Thermal conductivity of fluid
v_{nf}	Nanofluid kinematic viscosity
v_f	Fluid kinematic viscosity
T_∞	Ambient temperature
T_w	Wall temperature
ρ	Density
N_1	Angular velocity along X-direction
N_2	Angular velocity along Y-direction
F	Velocity profile along X-direction
g	Velocity profile along Y-direction
θ	Temperature profile
K	Micro-polar parameter
n	Micro-gyration parameter
ϕ	Nanoparticle volume fraction
Pr	Prandtl number
Nu	Nusselt number

Subscripts

f	Base fluid
nf	Nanofluid
w	Wall
hnf	Hybrid nanofluid
$s1$	First nanoparticle
$s2$	Second nanoparticle

Introduction

It can be observed from the studies in the past few years that nanofluids have an important role in many engineering operations due to their significant effect on fluids characteristics. One of the most effective ways to improve the thermal conductivity of fluid is dispersing nanoparticles into it. Each nanometer-sized carbon, crystal, metal, and other related elements give various traits and different ranges of thermal conductivity to the base fluid when they are poured in it. Base fluids can be water, oil, biofluid, or any fluid used in engineering operations. There are many studies around different aspects of nanofluids behavior. In the beginning, Choi [1] observed Changes in heat transfer rate by adding nanoparticles into water. Eastman et al. [2] studied ethylene glycol with 0.3% volume copper nanoparticles and witnessed a 40% growth in effective thermal conductivity. 10–30% enhance in thermal conductivity in alumina/water nanofluid has been resulted in Das et al. research [3]. Volume fraction, shape, and size of nanoparticles are also key factors of their efficiency. The magnetic field also improves some nanofluid's thermal conductance. Tiwari and das [4] studied the effect of solid volume fraction, viscosity and particle size on nanofluids heat transfer improvement.

Magnetohydrodynamic includes magnetic field, liquid and movement of the particles and is one of the frequently researched subjects in heat transfer processes. Ellahi [5] investigated the motion decrement of a non-newtonian MHD flow in a pipe by changing the MHD

parameters. Mansur et al. [6] studied magnetohydrodynamics (MHD) homogeneous reaction, made by a penetrable shrinking sheet in a Nanofluid flow. The effects of MHD on the flows that contain Ferro fluid as the operative fluid is examined by Ganji and sheikholeslami [7]. MHD flow due to stretching surfaces is studied by Akram et al. [8] Other researches around nanofluids are shown in Refs. [9–15].

Eringen [16] introduced the micropolar fluid. The physical properties and their usages were studied by Lukaszewicz [17]. He studied fluid molecules randomly orientin whicheach volume fluid element has its rotation and translation motions. Analysis of these fluids gave different results than newtonian fluids. Kumar et al. [18] examined the investigated laminar flow of the micropolar fluids in a vertical channel which resulted in an impressive impact of fluid parameters on the velocity profile. Magneto-micropolar flow enhanced with nanoparticle under stagnation point zone is studied by Rashidi et al. [19]. Other recent studies around MHD micropolar nanofluid are addressed in Refs. [20–23].

In recent years there were widespread studies around curvy enclosures with various shapes and geometries due to the major effect of their geometry on heat transfer rate. These kinds of enclosures have a tremendous engineering application and are commonly utilized in heat exchangers and cooling systems. In this study, thesinusoidal cylinder has been used as a wavy enclosure. Sheikholeslami [24] investigated the effect of electrical field on nanofluids viscosity inside a container with sinusoidal walls which electrical field resulted in an improvement in convective heat transfer rate. Heat transfer and water flow with CU–O nanoparticles inside a porous intricate-shaped container have been studied by Sheikholeslami and Rokni [25] in presence of MHD field. Sheikholeslami [26] also studied the effect of electrical field on water with Cu3O4 nanoparticles in an enclosure with horizontally moving lower wall and fixed sinusoidal upper wall. It resulted that Different voltage rates make different streamlines. Quarter-circular container with inner and outer sinusoidal walls was discussed by Tang et al. [27] and depicted a big effect of nanofluids volume fraction on Nusselt number. Natural convection with different boundary conditions in a curvy container is studied numerically by Oztop et al. [28, 29]. more researches around enclosures with various geometries and condition are shown in Refs. [30–39]

The Mathematical Formulation of the Problem

Figure 1 presents the geometry of the problem (stagnation points are depicted as M, N, and O) in which a steady micropolar nanofluid flow, in the presence of a magnetic field, past over a sinusoidal cylinder.

Base fluid is a mixture of ethylene glycol and water ($C_2H_6O_2$–H_2O) and nanoparticles are iron oxide (Fe_3O_4) and Molybdenum disulfide(MoS_2) which properties are presented in Table 1. For such a problem equations are as follow [17]:

the continuity equation is as follows:

$$\frac{\partial U}{\partial x} + \frac{\partial V}{\partial y} + \frac{\partial W}{\partial z} = 0 \qquad (1)$$

Momentum equations in alignment with flow direction and perpendicular to it are as follow, respectively:

$$U\frac{\partial U}{\partial x} + V\frac{\partial U}{\partial y} + W\frac{\partial U}{\partial z} = a^2 x + \left(\frac{\mu_{nf} + k}{\rho_{nf}}\right)\frac{\partial^2 U}{\partial^2 z} + \frac{k}{\rho_{nf}}\frac{\partial N_2}{\partial z} + \frac{\sigma B_\circ^2}{\rho_{nf}}(U - ax) \quad (2)$$
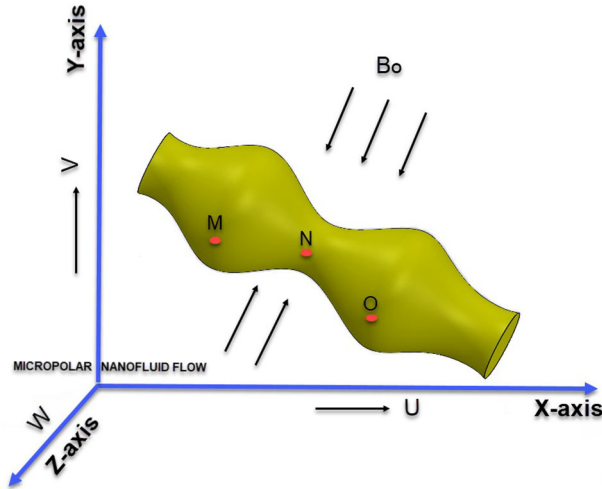
210 Page 4 of 17

Int. J. Appl. Comput. Math (2021) 7:210

Fig. 1 Geometry of the problem

Table 1 Thermophysical properties ofbase fluid and nanoparticle [48]

Physical properties	$C_2H_6O_2$–H_2O	Fe_3O_4	MoS_2
$\rho\left(\frac{kg}{m^3}\right)$	1063.8	5180	5060
$C_p\left(\frac{J}{kg.^{\circ}K}\right)$	3630	670	397.21
$k\left(\frac{W}{m.^{\circ}K}\right)$	0.387	9.7	904.4

$$U\frac{\partial V}{\partial x} + V\frac{\partial V}{\partial y} + W\frac{\partial V}{\partial z} = b^2 x + \left(\frac{\mu_{nf} + k}{\rho_{nf}}\right)\frac{\partial^2 V}{\partial^2 z} - \frac{k}{\rho_{nf}}\frac{\partial N_1}{\partial z} + \frac{\sigma B_\circ^2}{\rho_{nf}}(V - by) \quad (3)$$

Energy equation is as follow:

$$U\frac{\partial T}{\partial x} + V\frac{\partial T}{\partial y} + W\frac{\partial T}{\partial z} = \alpha_{nf}\frac{\partial^2 T}{\partial^2 z} \quad (4)$$

Angular momentum conservation for mentioned flow will end up to following statements:

$$U\frac{\partial N_1}{\partial x} + V\frac{\partial N_1}{\partial y} + W\frac{\partial N_1}{\partial z} = \frac{1}{\rho_{nf}} + \left(\mu_{nf}\frac{k}{2}\right)\frac{\partial^2 N_1}{\partial^2 z} - \frac{2k}{j\rho_{nf}}\frac{\partial V}{\partial z} - \frac{2k}{j\rho_{nf}}N_1 \quad (5)$$

$$U\frac{\partial N_2}{\partial x} + V\frac{\partial N_2}{\partial y} + W\frac{\partial N_2}{\partial z} = \frac{1}{\rho_{nf}} + \left(\mu_{nf}\frac{k}{2}\right)\frac{\partial^2 N_2}{\partial^2 z} + \frac{2k}{j\rho_{nf}}\frac{\partial U}{\partial z} - \frac{2k}{j\rho_{nf}}N_2 \quad (6)$$

The boundary conditions are as follow:

$$V = 0, U = 0, W = 0, N_1 = n\frac{\partial V}{\partial z}, N_2 = -n\frac{\partial U}{\partial z}, T = T_w \text{ at } z \to 0$$

$$U \to ax, V \to by, T \to T_\infty, N_1 \to 0, N_2 \to 0 \text{ at } z \to 0 \quad (7)$$

Int. J. Appl. Comput. Math (2021) 7:210

Page 5 of 17   **210**

Implementing Bachok et al. [40] methodology for finding the physical quantity of hybrid nanoflow ended up to the following results (physical quantity for individual material are presented in Table 1).

$$(1 - \phi_1)^{2.5}(1 - \phi_2)^{2.5} = \frac{\mu_f}{\mu_{hnf}}$$

$$k_{bf} = k_f \left(\frac{k_{s1} + (s-1)k_f - (s-1)\phi_1(k_f - k_{s1})}{k_{s1} + (s-1)k_f + \phi_1(k_f - k_{s1})} \right)$$

$$k_{hnf} = k_{bf} \left(\frac{k_{s2} + (s-1)k_{bf} - (s-1)\phi_2(k_{bf} - k_{s2})}{k_{s2} + (s-1)k_{bf} + \phi_2(k_{bf} - k_{s2})} \right)$$

$$\rho_{hnf} = \rho_f (1 - \phi_2)\left((1 - \phi_1) + \phi_1\left(\frac{\rho_{s1}}{\rho_f} \right) \right) + \phi_2 \rho_{s2}$$

$$(\rho c_p)_{hnf} = (\rho c_p)_f (1 - \phi_2)\left((1 - \phi_1) + \phi_1\frac{(\rho c_p)_{s1}}{(\rho c_p)_f} \right) + \phi_2(\rho c_p)_{s2}$$

$$\alpha_{hnf} = \frac{k_{hnf}}{(\rho c_p)_{hnf}}$$

$$\Pr = \frac{\nu}{\alpha} \tag{8}$$

Following similarity are considered to normalize the equations.

$$U = axf'(\eta), \ V = byg'(\eta), \ W = -\sqrt{a\nu_f}(f + cg), \ T = T_\infty + (T_w + T_\infty)\theta(\eta),$$

$$\eta = z\sqrt{\frac{\nu_f}{a}}, \ N_1 = by\sqrt{\frac{a}{\nu_f}}h(\eta), \ N_2 = ax\sqrt{\frac{a}{\nu_f}}\psi(\eta) \tag{9}$$

By applying the aforementioned similarities, the partial equations transform into the following ordinary equations:

$$\left(\frac{1}{\left((1 - \phi_2)\left((1 - \phi_1) + \frac{(\rho_{s1})}{(\rho_f)}\phi_1 \right) + \frac{\phi_2(\rho_{s2})}{(\rho_f)} \right)} \right)$$

$$\left(\frac{1}{(1 - \phi_1)^{2.5}(1 - \phi_2)^{2.5}} + K \right) f''' + (f + cg)f'' - f'^2$$

$$+ \left(\frac{K}{\left((1 - \phi_2)\left((1 - \phi_1) + \frac{(\rho_{s1})}{(\rho_f)}\phi_1 \right) + \frac{\phi_2(\rho_{s2})}{(\rho_f)} \right)} \right) \psi'$$

$$- \left(\frac{M^2}{\left((1 - \phi_2)\left((1 - \phi_1) + \frac{(\rho_{s1})}{(\rho_f)}\phi_1 \right) + \frac{\phi_2(\rho_{s2})}{(\rho_f)} \right)} \right)(f' - 1) + 1 = 0 \tag{10}$$

$$\left(\frac{1}{\left((1 - \phi_2)\left((1 - \phi_1) + \frac{(\rho_{s1})}{(\rho_f)}\phi_1 \right) + \frac{\phi_2(\rho_{s2})}{(\rho_f)} \right)} \right)$$

$$\left(\frac{1}{(1 - \phi_1)^{2.5}(1 - \phi_2)^{2.5}} + K \right) g''' + (f + cg)g'' - cg'^2$$

$$-\left(\frac{K}{\left((1-\phi_2)\left((1-\phi_1)+\frac{(\rho_{s1})}{(\rho_f)}\phi_1\right)+\frac{\phi_2(\rho_{s2})}{(\rho_f)}\right)}\right)h'$$

$$-\left(\frac{M^2}{\left((1-\phi_2)\left((1-\phi_1)+\frac{(\rho_{s1})}{(\rho_f)}\phi_1\right)+\frac{\phi_2(\rho_{s2})}{(\rho_f)}\right)}\right)(f'-1)+c=0 \qquad (11)$$

$$\left(\frac{\frac{k_{hnf}}{k_f}}{\Pr\left((1-\phi_2)\left((1-\phi_1)+\frac{(\rho c_p)_{s1}}{(\rho c_p)_f}\phi_1\right)+\frac{\phi_2(\rho c_p)_{s2}}{(\rho c_p)_f}\right)}\right)\theta''+(f+cg)\theta'=0 \qquad (12)$$

$$\left(\frac{1}{\left((1-\phi_2)\left((1-\phi_1)+\frac{(\rho_{s1})}{(\rho_f)}\phi_1\right)+\frac{\phi_2(\rho_{s2})}{(\rho_f)}\right)}\right)$$

$$\left(\frac{1}{(1-\phi_1)^{2.5}(1-\phi_2)^{2.5}}+\frac{K}{2}\right)h''+(f+cg)h'$$

$$-\left(\frac{2K}{\left((1-\phi_2)\left((1-\phi_1)+\frac{(\rho_{s1})}{(\rho_f)}\phi_1\right)+\frac{\phi_2(\rho_{s2})}{(\rho_f)}\right)}\right)h$$

$$-\left(\frac{K}{\left((1-\phi_2)\left((1-\phi_1)+\frac{(\rho_{s1})}{(\rho_f)}\phi_1\right)+\frac{\phi_2(\rho_{s2})}{(\rho_f)}\right)}\right)g''+cg'h=0 \qquad (13)$$

$$\left(\frac{1}{\left((1-\phi_2)\left((1-\phi_1)+\frac{(\rho_{s1})}{(\rho_f)}\phi_1\right)+\frac{\phi_2(\rho_{s2})}{(\rho_f)}\right)}\right)$$

$$\left(\frac{1}{(1-\phi_1)^{2.5}(1-\phi_2)^{2.5}}+\frac{K}{2}\right)\psi''+(f+cg)\psi'$$

$$-\left(\frac{2K}{\left((1-\phi_2)\left((1-\phi_1)+\frac{(\rho_{s1})}{(\rho_f)}\phi_1\right)+\frac{\phi_2(\rho_{s2})}{(\rho_f)}\right)}\right)\psi$$

$$+\left(\frac{K}{\left((1-\phi_2)\left((1-\phi_1)+\frac{(\rho_{s1})}{(\rho_f)}\phi_1\right)+\frac{\phi_2(\rho_{s2})}{(\rho_f)}\right)}\right)f''+f'\psi=0 \qquad (14)$$

After transforming the equations, boundary conditions turn into the following statement:

$$\begin{cases} f(0)=f'(0)=0 \\ g(0)=g'(0)=0 \\ \theta(0)=g'(\infty)=f'(\infty)=1 \\ h(0)=ng''(0),\ \psi(0)=-nf''(0) \\ \psi(\infty)=h(\infty)=\theta(\infty)=0 \end{cases} \qquad (15)$$

In which "f'", "g'" are the velocity profiles in "X" and "Y" direction, respectively; "θ" is the temperature profile; "ψ" is the micropolar profile along Y-axis and "h" is the micropolar profile perpendicular to Y-axis.

$K = \frac{K}{\mu_f}$ is the micropolar parameter; $M = \frac{\sigma B_0^2}{a \rho_f}$ is the magnetic filed and $c = \frac{a}{b}$ is the ratioparameter.

Nusselt number and skin friction coefficient are as follow:

$$C_{fx} = \frac{\tau_{wx}}{\rho_f u_w^2}, \, C_{fy} = \frac{\tau_{wy}}{\rho_f u_w^2}, \, Nu = \frac{xq_w}{k_f(T_w - T_\infty)} \tag{16}$$

Shear stress along X and Y direction are presented in the following statement:

$$\tau_{wx} = \left[(\mu_{hnf} + k) \frac{\partial U}{\partial z} k N_2 \right]_{z=0},$$

$$\tau_{wy} = \left[(\mu_{hnf} + k) \frac{\partial V}{\partial z} k N_1 \right]_{z=0}, \, q_w = -k_{hnf} \left(\frac{\partial T}{\partial z} \right)_{z=0} \tag{17}$$

$$\mathrm{Re}_x^{1/2} C_{fx} = \left(\frac{1}{(1 - \phi_1)^{2.5}(1 - \phi_2)^{2.5}} + K(1 - n) \right) f''(0) \tag{18}$$

$$(x/y)\mathrm{Re}_x^{-1/2} C_{fy} = c \left(\frac{1}{(1 - \phi_1)^{2.5}(1 - \phi_2)^{2.5}} + (1 + n)K \right) g''(0) \tag{19}$$

$$\mathrm{Re}_x^{-1/2} Nu_x = -\frac{k_{hnf}}{k_f} \theta'(0) \tag{20}$$

Numerical Procedure

The equations in later part transformed from PDEs to nonlinear ODEs, then by taking advantage of theMAPELsoftware the Rung-Kutta fifth-order is applied to solve the nonlinear ODEs. To do that some steps must be taken.First, thenonlinearordinary differentialequations have to be transformed into a system of 1st-order differential equations. Therefore, new sets of variables are defined as follow:

$$f = O_1, f' = O_1' = O_2, f'' = O_2' = O_3, g = O_4, g' = O_4' = O_5, g'' = O_5' = O_6$$
$$\theta = O_7, \theta' = O_7' = O_8, h = O_9, h' = O_9' = O_{10}, \psi = O_{11}, \psi' = O_{11}' = O_{12}. \tag{21}$$

Second, the variables (21) substitute into Eqs. (10–14), this will end up to the following system of ODEs:

$$
\begin{pmatrix} O_1' \\ O_2' \\ O_3' \\ O_4' \\ O_5' \\ O_6' \\ O_7' \\ O_8' \\ O_9' \\ O_{10}' \\ O_{11}' \\ O_{12}' \end{pmatrix} =
\begin{pmatrix}
O_2 \\
O_3 \\
\left(\dfrac{1}{\left((1-\phi_2)\left((1-\phi_1)+\frac{(\rho_{s1})}{(\rho_f)}\phi_1 \right)+\frac{\phi_2(\rho_{s2})}{(\rho_f)} \right)} \right) \left(\dfrac{1}{(1-\phi_1)^{2.5}(1-\phi_2)^{2.5}} + K \right) + (O_1 + cO_4)O_3 - O_2{}^2 \\
\quad + \left(\dfrac{K}{\left((1-\phi_2)\left((1-\phi_1)+\frac{(\rho_{s1})}{(\rho_f)}\phi_1 \right)+\frac{\phi_2(\rho_{s2})}{(\rho_f)} \right)} \right) O_{12} - \left(\dfrac{M^2}{\left((1-\phi_2)\left((1-\phi_1)+\frac{(\rho_{s1})}{(\rho_f)}\phi_1 \right)+\frac{\phi_2(\rho_{s2})}{(\rho_f)} \right)} \right)(O_2 - 1) + 1 = 0 \\
O_5 \\
O_6 \\
\left(\dfrac{1}{\left((1-\phi_2)\left((1-\phi_1)+\frac{(\rho_{s1})}{(\rho_f)}\phi_1 \right)+\frac{\phi_2(\rho_{s2})}{(\rho_f)} \right)} \right) \left(\dfrac{1}{(1-\phi_1)^{2.5}(1-\phi_2)^{2.5}} + K \right) + (O_1 + cO_4)O_6 - cO_5{}^2 \\
\quad - \left(\dfrac{K}{\left((1-\phi_2)\left((1-\phi_1)+\frac{(\rho_{s1})}{(\rho_f)}\phi_1 \right)+\frac{\phi_2(\rho_{s2})}{(\rho_f)} \right)} \right) O_{10} - \left(\dfrac{M^2}{\left((1-\phi_2)\left((1-\phi_1)+\frac{(\rho_{s1})}{(\rho_f)}\phi_1 \right)+\frac{\phi_2(\rho_{s2})}{(\rho_f)} \right)} \right)(O_2 - 1) + c = 0 \\
O_8 \\
\left(\dfrac{\frac{k_{hnf}}{k_f}}{\Pr\left((1-\phi_2)\left((1-\phi_1)+\frac{(\rho c_p)_{s1}}{(\rho c_p)_f}\phi_1 \right)+\frac{\phi_2(\rho c_p)_{s2}}{(\rho c_p)_f} \right)} \right) + (O_1 + cO_4)O_8 = 0 \\
O_{10} \\
\left(\dfrac{1}{\left((1-\phi_2)\left((1-\phi_1)+\frac{(\rho_{s1})}{(\rho_f)}\phi_1 \right)+\frac{\phi_2(\rho_{s2})}{(\rho_f)} \right)} \right) \left(\dfrac{1}{(1-\phi_1)^{2.5}(1-\phi_2)^{2.5}} + \frac{K}{2} \right) + (O_1 + cO_4)O_{10} \\
\quad - \left(\dfrac{2K}{\left((1-\phi_2)\left((1-\phi_1)+\frac{(\rho_{s1})}{(\rho_f)}\phi_1 \right)+\frac{\phi_2(\rho_{s2})}{(\rho_f)} \right)} \right) O_9 - \left(\dfrac{K}{\left((1-\phi_2)\left((1-\phi_1)+\frac{(\rho_{s1})}{(\rho_f)}\phi_1 \right)+\frac{\phi_2(\rho_{s2})}{(\rho_f)} \right)} \right) O_6 + cO_5 O_9 = 0 \\
O_{12} \\
\left(\dfrac{1}{\left((1-\phi_2)\left((1-\phi_1)+\frac{(\rho_{s1})}{(\rho_f)}\phi_1 \right)+\frac{\phi_2(\rho_{s2})}{(\rho_f)} \right)} \right) \left(\dfrac{1}{(1-\phi_1)^{2.5}(1-\phi_2)^{2.5}} + \frac{K}{2} \right) + (O_1 + cO_4)O_{12} \\
\quad - \left(\dfrac{2K}{\left((1-\phi_2)\left((1-\phi_1)+\frac{(\rho_{s1})}{(\rho_f)}\phi_1 \right)+\frac{\phi_2(\rho_{s2})}{(\rho_f)} \right)} \right) O_{11} + \left(\dfrac{K}{\left((1-\phi_2)\left((1-\phi_1)+\frac{(\rho_{s1})}{(\rho_f)}\phi_1 \right)+\frac{\phi_2(\rho_{s2})}{(\rho_f)} \right)} \right) O_3 + O_2 O_{11} = 0
\end{pmatrix}
\tag{22}
$$

Third, the boundary conditions should convert:

$$
\begin{pmatrix} O_1(0) \\ O_2(0) \\ O_2(\infty) \\ O_4(0) \\ O_5(0) \\ O_5(\infty) \\ O_7(0) \\ O_7(\infty) \\ O_9(0) \\ O_9(\infty) \\ O_{11}(0) \\ O_{11}(\infty) \end{pmatrix} =
\begin{pmatrix} 0 \\ 0 \\ 1 \\ 0 \\ 0 \\ 1 \\ 1 \\ 0 \\ nO_6(0) \\ 0 \\ -nO_3(0) \\ 0 \end{pmatrix}
\tag{23}
$$

Now we can solve these equations by taking followingprecondition:

It good to notice that after iterating calculation for various η,four is considered instead ofinfinity ($\eta \to \infty$), since the effect of parameters are worn off after four.

Results and Discussion

In the current study, micropolar nanofluid flow across sinusoidal cylinder in presence of magnetic field is investigated. The generic equation is transformed from partial to ordinary type and Runge–Kutta fifth-order is applied to solve ODEs. The impact of various parameter e.g., micro-polar parameter(k), nanoparticle volume fraction (ϕ), magnetic field parameter(M), shape factor(s) are studied.The validation is done based on the result of Kh.Hosseinzadeh et al. [41] and comparison is presented in Fig. 2.

Figure 3 depicts velocity profiles alongside the Xand Yaxises. In Fig. 3a effect of themicropolar parameter(k) and micro-gyration parameter (n)is shown. It can be said thatboth "n" and "k" have reverse relation with velocity profile. Bhattacharyya [42] and Wang [43] show that for k = 0 fluid behave likenewtonian flow. In micropolar fluid flow (k > 0), the micro rotation affects the flow field and, as it's shown, by increasing k, the velocity profile decreases.In this study, two different scenarios for "n" are analyzed, firstly n = 0 (black color) belongs to the high concentration of microelements close to the wall. In this case, microelements in the vicinity of the wall are kind of disable to rotate. Secondly, n > 1 (red color) corresponds to the low concentration of microelements at the wall, so in this case, rotation can happen [44].

Figure 3b shows the impact of various volume fractions on the velocity profile (F'). It seems that F' is an increasing function of both micro-gyration and nanoparticle volume fraction. Figure 3c represents the effect of different magnetic field parameters on F'.In presence of the magnetic field electric vorties are generated[45]. These vortices have a dissiapantnuture, they dissipate enegy and prevent increment of velocity, therefore the velocity profiles decrease by increasing the magnetic field.
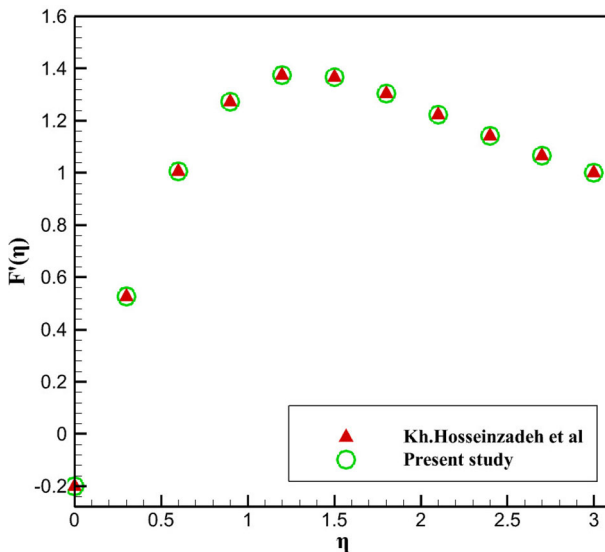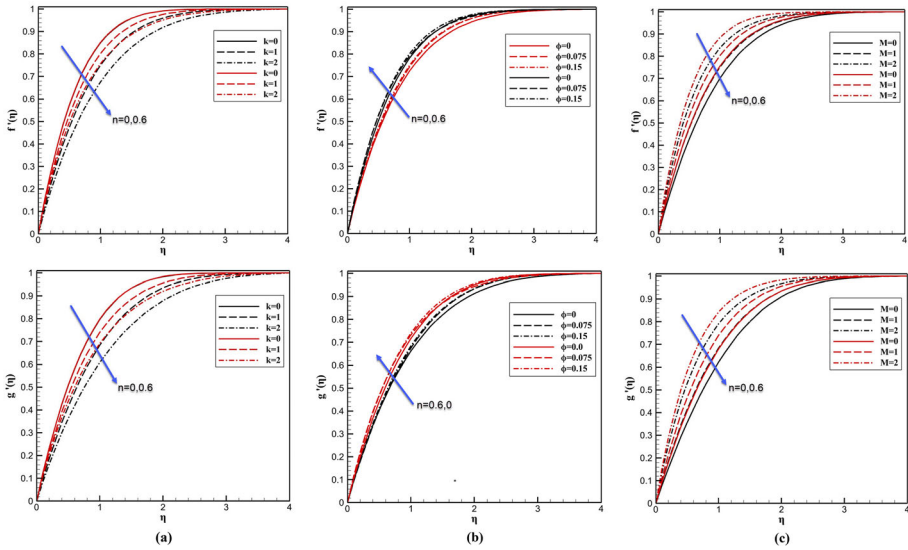

Fig. 2 validation of current study based on the result of Kh.Hosseinzadeh et al. [41]

Fig. 3 Velocity profile along X and Y directions with respect to the micro-gyration parameter for **a** different micro-polar parameter, **b** different nanoparticle volume fraction and **c** different magnetic field parameter

Figure 4 presents the effect of different shape factors and different nanoparticle volume fractions on the temperature profile. Figure 4a shows that this profile is an increasing function ofshape factor. In Table 2, values of shape factor are shown. On the other hand, by increasing the micro-gyration parameter the temperature profile falls. In Fig. 4b effect of volume fraction on the temperatureprofile is shown. This profile sees increment by an increase in both the micro-gyration parameter and volume fraction. Physically, increment in volume fraction leads to a highr thermal conductivity that implies a higher rate of heat transfer and higher temperature. The volume fraction is defined as "a constituent of a mixture divided by the sum of volumes of all constituents prior to mixing"[46].

Nanoparticles have a higher thermal conductivity than base fluid, therefore by adding nanoparticles (increasing volume fraction) the hybridized flow has more potential to reach a higher temperature.

Figure 5 shows the effect of different micro-polar parameters, different nanoparticle volume fractions and different magnetic field parameters on the micropolar profile along Xand-Yaxises("h" and "ψ", respectively). Figure 5a, b show that "h" and "ψ" treat opposite each other. "h" is an increasing function of micro-gyration parameter, volume fraction and magnetic field but a decreasing function of the micro-polar parameter,on the other hand, ψ is a decreasing function of what mentioned for h with only one exception:the electric vortices effect only in one direction, and that direction is along "h".

Figure 6 outlinestheeffect of different magnetic field parameters "M", different micro-polar parameters "K"and different nanoparticle volume fractions "ϕ" on Nu number and skin friction coefficient.

As it's shown in Fig. 6a, b, by increasing the magnetic field the electric vortices grow, therefore these vortices resist against the flow. Since such a treatment increases friction, it can be saide that this resistance leads to an increase in the skin friction coefficient. Because, when resistance happened, as mentioned above, the velocity will decrease. By decreasing
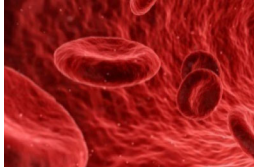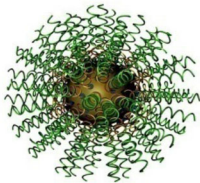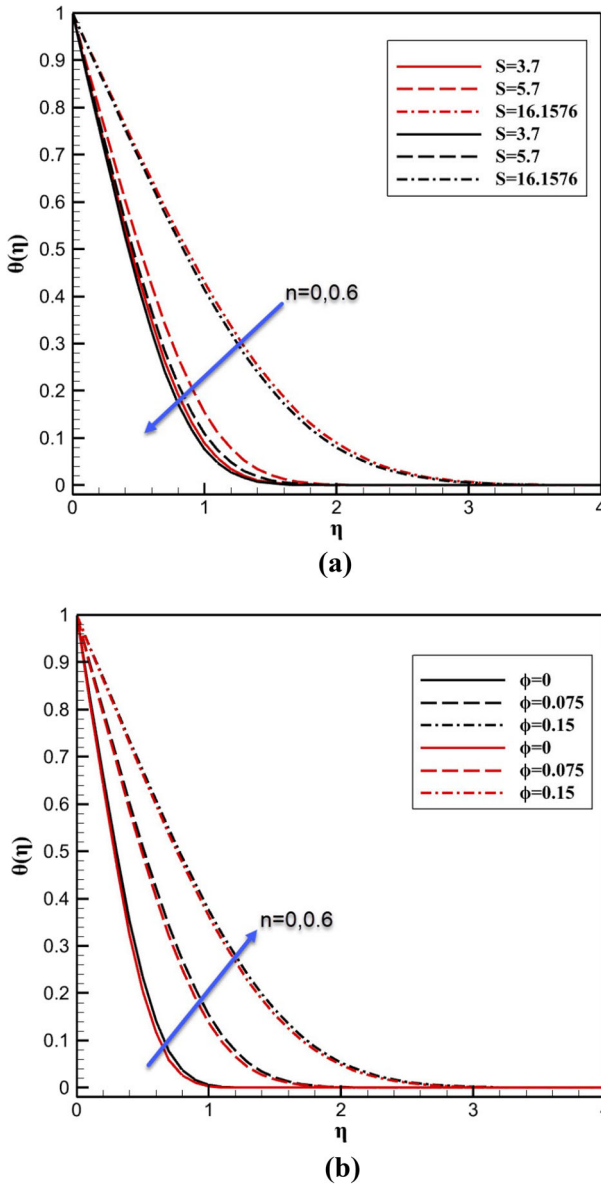
Fig. 4 Temperature profile with respect to the micro-gyration parameter for **a** different shape factor **b** different nanoparticle volume fraction

the velocity (note to Eq. 18) Re number will fall. Due to the reverse relation between Cf and Re, any kind of decrement in Re number will end up to a greater Cf.

A higher nanoparticle volume fraction leads to higher thermal conductivity[47]. Equations (16–20) describe that the Nu number is an increasing function of Re number but a decreasing function of thermal conductivity. From Fig. 6d, it can be deduced that the Nu number is in harmony with nanoparticle volume fraction. To describe this treatment,based on

Table 2 Shape factor coefficient for different nanoparticles'shapes [49]

| Types of nanoparticles	Shape	Shape factor
Bricks		S = 3.7
Platelets		S = 5.7
Lamina		S = 16.1576

Eq. (20), numerical sensitivity analysis is presented in Table 3, for various volume fractions. This equation tells that the Nu number divided by the square root of Re is a multiplication of $\theta'(0)$ by $-\frac{k_{hnf}}{k_f}$. Table 3 shows that the increment in the ratio of thermal conductivities is so much greater than the reduction in $\theta'(0)$.

Conclusion

This research tried to covermicropolar nanofluid flow across sinusoidal cylinders in presence of magnetic field Besides the consequence of various parametersareare investigated: the micro-gyration parameter, micro-polar parameter, nanoparticle volume fraction and magnetic field parameter. The outcomes of this study indicate thatwhenthemicro-gyrationis zero the microelements near to wall are unable to rotate and by increasing themicro-gyration parameters these microelements will rotate. The velocity profiles are increasing function of the volume fraction, while they decreased by themicro-polar parameter and magnetic the-field parameter. The temperature profile is an increasing function of both volume fraction and shape factor. The micropolr prameter along X and Y direction treat opposite each other. By empowering the magnetic field (increasing the electric vortices) skin friction coefficient will grow. Thou increasing volume fraction leads to greater Nu number.
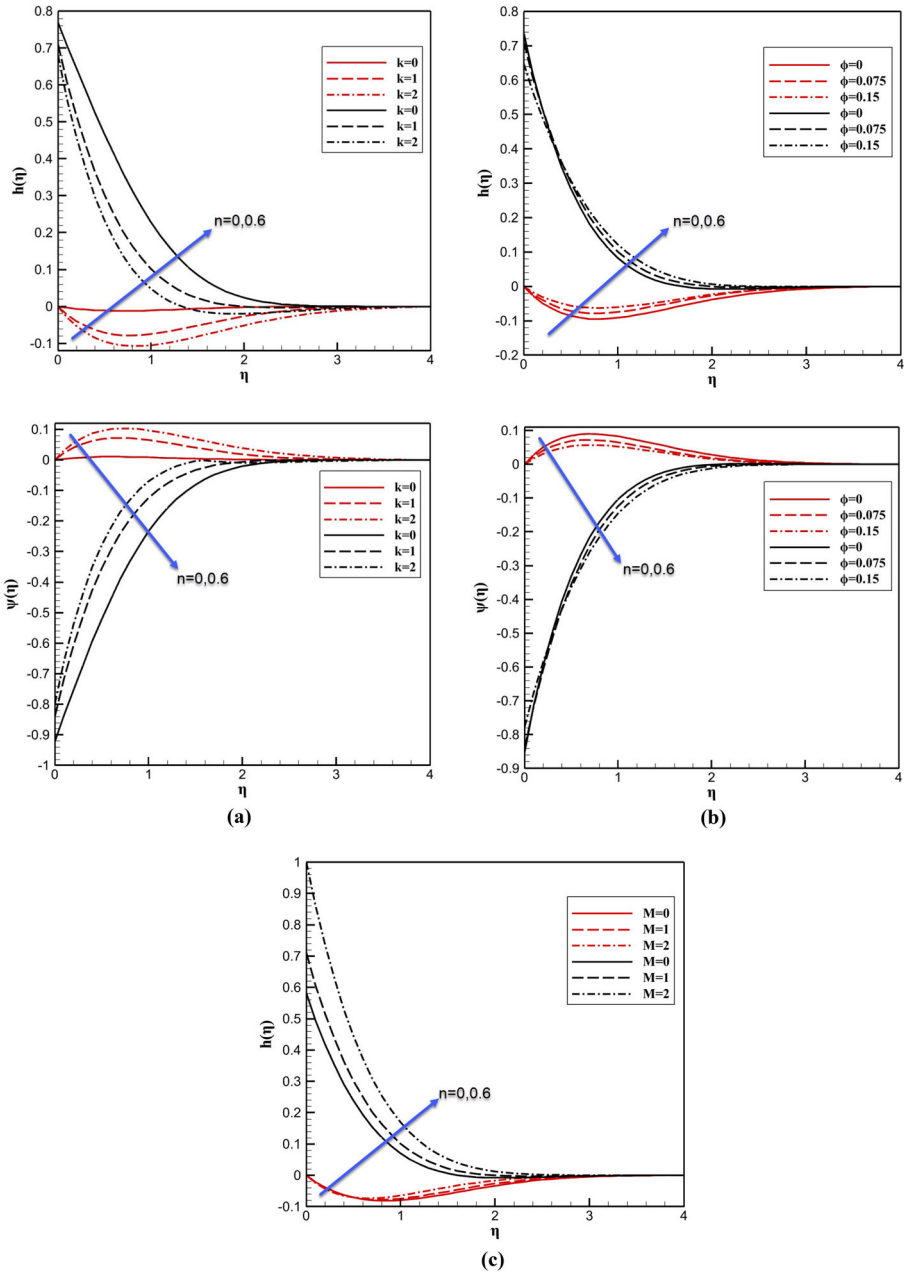
Fig. 5 micropolar profile along X-axis andY-axis ("h" and "ψ", respectively)with respect to micro-gyration parameter for **a** different micro-polar parameter, **b** different nanoparticle volume fraction and **c** different magnetic field parameter
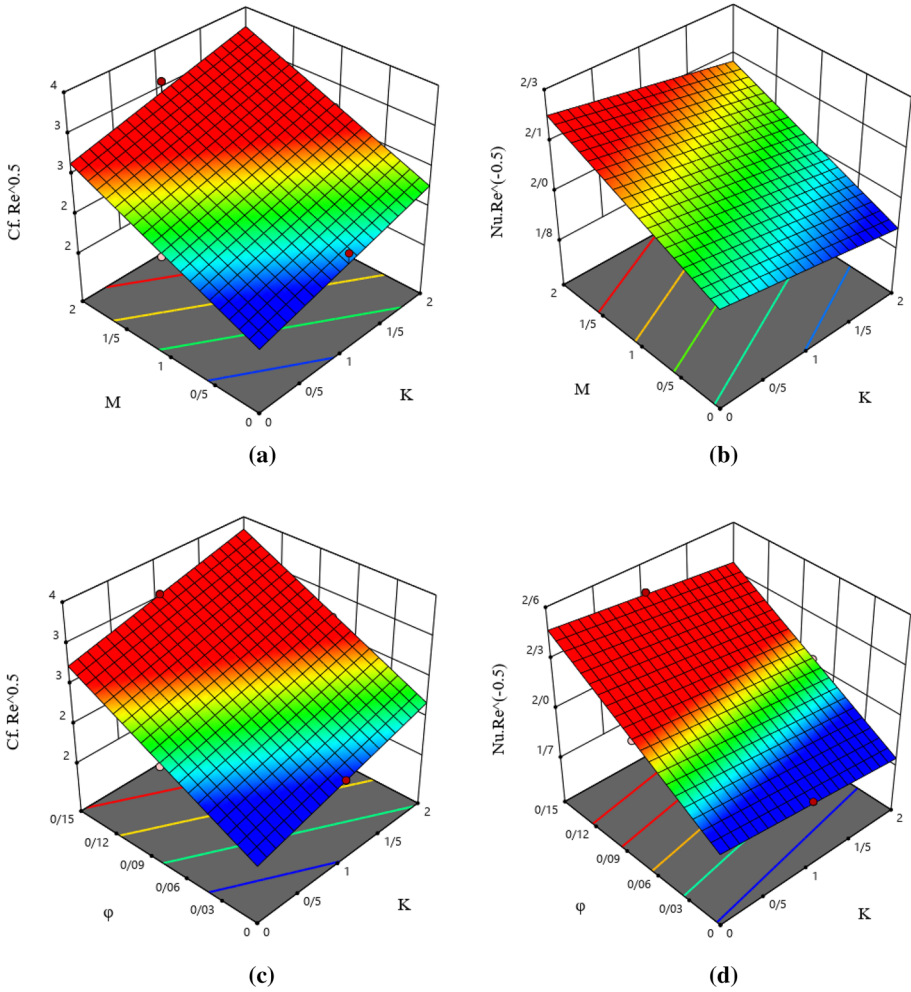
Fig. 6 variation of skin friction coefficient (cf) and Nusselt number (Nu) by different magnetic field parameter "M", different micro-polar parameter "K" and different nanoparticle volume fraction "ϕ"

Table 3 sensitivity analysis based on various volume fraction

ϕ	$\theta'(0)$	$-\dfrac{k_{hnf}}{k_f}$	$\dfrac{Nu_x}{\sqrt{Re_x}}$
0	-1.80955172904318	-1.000000000	1.809551729
0.075	-1.04602201992296	-1.997882009	2.089828575
0.15	-0.679164990176892	-3.574672145	2.427792172

Declarations

Conflict of interest The authors don't have any conflict of interest.

References

1. Choi, S.U., Eastman, J.A.: Enhancing Thermal Conductivity of Fluids with Nanoparticles. Argonne National Lab, Lemont (1995)
2. Eastman, J.A., Choi, S.U., Li, S., Yu, W., Thompson, L.J.: Anomalously increased effective thermal conductivities of ethylene glycol-based nanofluids containing copper nanoparticles. Appl. Phys. Lett. **78**(6), 718–720 (2001)
3. Das, S.K., Putra, N., Thiesen, P., Roetzel, W.: Temperature dependence of thermalconductivity enhancement for nanofluids. ASME J. Heat Transf. **125**, 567–574 (2003)
4. Xuan, Y., Li, Q.: Investigation on convective heat transfer and flow features of nanofluids. J. Heat transfer. **125**(1), 151–155 (2003)
5. Mansur, S., Ishak, A., Pop, I.: MHD homogeneous-heterogeneous reactions in a nanofluid due to a permeable shrinking surface. J. Appl. Fluid Mech. **9**(3), 1073–1079 (2016)
6. Ellahi, R.: The effects of MHD and temperature dependent viscosity on the flow of non-Newtonian nanofluid in a pipe: analytical solutions. Appl. Math. Model. **37**(3), 1451–1467 (2013)
7. Sheikholeslami, M., Ganji, D.D.: Ferrohydrodynamic and magnetohydrodynamic effects on ferrofluid flow and convective heat transfer. Energy **75**, 400–410 (2014)
8. Akram, S., Zafar, M., Nadeem, S.: Peristaltic transport of a Jeffrey fluid with double-diffusive convection in nanofluids in the presence of inclined magnetic field. Int. J. Geometric Methods Mod. Phys. **15**(11), 1850181 (2018)
9. Hayat, T., Javed, M., Imtiaz, M., Alsaedi, A.: Convective flow of Jeffrey nanofluid due to two stretchable rotating disks. J. Mol. Liq. **240**, 291–302 (2017)
10. Hosseinzadeh, K., Moghaddam, M.E., Asadi, A., Mogharrebi, A.R., Jafari, B., Hasani, M.R., Ganji, D.D.: Effect of two different fins (longitudinal-tree like) and hybrid nano-particles (MoS_2-TiO_2) on solidification process in triplex latent heat thermal energy storage system. Alex. Eng. J. **60**(1), 1967–1979 (2021)
11. Jyothi, K., Reddy, P.S., Reddy, M.S.: Influence of magnetic field and thermal radiation on convective flow of SWCNTs-water and MWCNTs-water nanofluid between rotating stretchable disks with convective boundary conditions. Powder Technol. **331**, 326–337 (2018)
12. Khan, M.I., Hafeez, M.U., Hayat, T., Khan, M.I., Alsaedi, A.: Magneto rotating flow of hybrid nanofluid with entropy generation. Comput. Methods Progr. Biomed. **183**, 105093 (2020)
13. Hosseinzadeh, K., Asadi, A., Mogharrebi, A.R., Khalesi, J., Mousavisani, S., Ganji, D.D.: Entropy generation analysis of (CH2OH) 2 containing CNTs nanofluid flow under effect of MHD and thermal radiation. Case Stud. Thermal Eng. **14**, 100482 (2019)
14. Hosseinzadeh, K., Afsharpanah, F., Zamani, S., Gholinia, M., Ganji, D.D.: A numerical investigation on ethylene glycol-titanium dioxide nanofluid convective flow over a stretching sheet in presence of heat generation/absorption. Case Stud. Thermal Eng. **12**, 228–236 (2018)
15. Gholinia, M., Gholinia, S., Hosseinzadeh, K., Ganji, D.D.: Investigation on ethylene glycol nano fluid flow over a vertical permeable circular cylinder under effect of magnetic field. Res. Phys. **9**, 1525–1533 (2018)
16. Eringen, A.C.: Microcontinuum Field Theories: II. Fluent Media. Springer, Berlin (2001)
17. Lukaszewicz, G.: Micropolar Fluids: Theory and Applications. Springer, Berlin (1999)
18. Kumar, J.P., Umavathi, J.C., Chamkha, A.J., Pop, I.: Fully-developed free-convective flow of micropolar and viscous fluids in a vertical channel. Appl. Math. Model. **34**(5), 1175–1186 (2010)
19. Rashidi, M.M., Reza, M., Gupta, S.: MHD stagnation point flow of micropolar nanofluid between parallel porous plates with uniform blowing. Powder Technol. **301**, 876–885 (2016)
20. Mohsen, I., Mohammadi, S.A., Mehryan, S.A.M., Yang, T., Sheremet, M.A.: Thermogravitational convection of magnetic micropolar nanofluid with coupling between energy and angular momentum equations. Int. J. Heat Mass Transf. **145**, 118748 (2019)

210 Page 16 of 17

Int. J. Appl. Comput. Math (2021) 7:210

21. Gibanov, N.S., Sheremet, M.A., Pop, I.: Natural convection of micropolar fluid in a wavy differentially heated cavity. J. Mol. Liq. **221**, 518–525 (2016)

22. Sheremet, M.A., Pop, I., Ishak, A.: Time-dependent natural convection of micropolar fluid in a wavy triangular cavity. Int. J. Heat Mass Transf. **105**, 610–622 (2017)

23. Umavathi, J.C., Sheremet, M.A.: Onset of double-diffusive convection of a sparsely packed micropolar fluid in a porous medium layer saturated with a nanofluid. Microfluid. Nanofluid. **21**(7), 1–22 (2017)

24. Sheikholeslami, M., Rokni, H.B.: Influence of EFD viscosity on nanofluid forced convection in a cavity with sinusoidal wall. J. Mol. Liq. **232**, 390–395 (2017)

25. Sheikholeslami, M., Rokni, H.B.: Magnetohydrodynamic CuO–water nanofluid in a porous complex-shaped enclosure. J. Thermal Sci. Eng. Appl. **9**(4), 041007 (2017)

26. Sheikholeslami, M., Ellahi, R.: Electrohydrodynamic nanofluid hydrothermal treatment in an enclosure with sinusoidal upper wall. Appl. Sci. **5**(3), 294–306 (2015)

27. Tang, W., Hatami, M., Zhou, J., Jing, D.: Natural convection heat transfer in a nanofluid-filled cavity with double sinusoidal wavy walls of various phase deviations. Int. J. Heat Mass Transf. **115**, 430–440 (2017)

28. Öztop, H.F., Sakhrieh, A., Abu-Nada, E., Al-Salem, K.: Mixed convection of MHD flow in nanofluid filled and partially heated wavy walled lid-driven enclosure. Int. Commun. Heat Mass Transfer **86**, 42–51 (2017)

29. Öztop, H.F., Abu-Nada, E., Varol, Y., Chamkha, A.: Natural convection in wavy enclosure with volumetric heat sources [J]. Int. J. Therm. Sci. **50**(4), 502–514 (2011)

30. Sulochana, C., Ashwinkumar, G.P.: Impact of Brownian moment and thermophoresis on magnetohydrodynamic flow of magnetic nanofluid past an elongated sheet in the presence of thermal diffusion. Multidiscipl. Model. Mater. Struct. **14**, 744–755 (2018)

31. Mabood, F., Ashwinkumar, G.P., Sandeep, N.: Effect of nonlinear radiation on 3D unsteady MHD stagnancy flow of Fe_3O_4/graphene–water hybrid nanofluid. Int. J. Ambient Energy **2020**, 1–11 (2020)

32. Mabood, F., Ashwinkumar, G.P., Sandeep, N.: Simultaneous results for unsteady flow of MHD hybrid nanoliquid above a flat/slendering surface. J. Thermal Anal. Calorim. **146**, 227–239 (2020)

33. Ashwinkumar, G.P.: Heat and mass transfer analysis in unsteady MHD flow of aluminum alloy/silver-water nanoliquid due to an elongated surface. Heat Transf. **50**(2), 1679–1696 (2021)

34. Ashwinkumar, G.P., Sulochana, C., Samrat, S.P.: Effect of the aligned magnetic field on the boundary layer analysis of magnetic-nanofluid over a semi-infinite vertical plate with ferrous nanoparticles. Multidiscipl. Model. Mater. Struct. **14**, 497–515 (2018)

35. Mohsen, I., Sheremet, M.A., Mehryan, S.A.M., Pop, I., Öztop, H.F., Abu-Hamdeh, N.: MHD thermogravitational convection and thermal radiation of a micropolar nanoliquid in a porous chamber. Int. Commun. Heat Mass Transf. **110**, 1409 (2020)

36. Hosseinzadeh, K., Mardani, M.R., Salehi, S., et al.: Entropy generation of three-dimensionalBödewadtflow of water and hexanol base fluid suspendedby Fe_3O_4 and MoS_2 hybrid nanoparticles. Pramana J. Phys. **95**, 57 (2021)

37. Mogharrebi, A.R., Ganji, A.R., Hosseinzadeh, K., Roghani, S., Asadi, A., Fazlollahtabar, A.: Investigation of magnetohydrodynamic nanofluid flow contain motile oxytactic microorganisms over rotating cone. Int. J. Numer. Methods Heat Fluid Flow (2021)

38. Gulzar, M.M., Aslam, A., Waqas, M., Javed, M.A., Hosseinzadeh, K.: A nonlinear mathematical analysis for magneto-hyperbolic-tangent liquid featuring simultaneous aspects of magnetic field, heat source and thermal stratification. Appl. Nanosci. **10**(12), 4513–4518 (2020)

39. Hosseinzadeh, K., Roghani, S., Mogharrebi, A.R., Asadi, A., Ganji, D.D.: Optimization of hybrid nanoparticles with mixture fluid flow in an octagonal porous medium by effect of radiation and magnetic field. J. Therm. Anal. Calorim. **19**, 1–2 (2020)

40. Bachok, N., Ishak, A., Nazar, R., Pop, I.: Flow and heat transfer at a general three-dimensional stagnation point in a nanofluid. Phys. B **405**(24), 4914–4918 (2010)

41. Hosseinzadeh, K., Salehi, S., Mardani, M.R., Mahmoudi, F.Y., Waqas, M., Ganji, D.D.: Investigation of nano-Bioconvective fluid motile microorganism and nanoparticle flow by considering MHD and thermal radiation. Inf. Med. Unlocked **21**, 100462 (2020)

42. Bhattacharyya, K.: Boundary layer flow and heat transfer over an exponentially shrinking sheet. Chin. Phys. Lett. **28**(7), 074701 (2011)

43. Miklavčič, M., Wang, C.: Viscous flow due to a shrinking sheet. Q. Appl. Math. **64**(2), 283–290 (2006)

44. Nazeer, M., Ali, N., Javed, T., Asghar, Z.: Natural convection through spherical particles of a micropolar fluid enclosed in a trapezoidal porous container. Eur. Phys. J. Plus **133**(10), 423 (2018)

45. Salehi, S., Nori, A., Hosseinzadeh, K., Ganji, D.D.: Hydrothermal analysis of MHD squeezing mixture fluid suspended by hybrid nanoparticles between two parallel plates. Case Stud. Thermal Eng. **21**, 100650 (2020)

46. McNaught, A.D.: Compendium of Chemical Terminology. Blackwell Science, Oxford (1997)

47. Masuda, H., Ebata, A., Teramae, K.: Alteration of thermal conductivity and viscosity of liquid by dispersing ultra-fine particles. Dispersion of Al_2O_3, SiO_2 and TiO_2 ultra-fine particles
48. Hosseinzadeh, K., Asadi, A., Mogharrebi, A.R., Azari, M.E., Ganji, D.D.: Investigation of mixture fluid suspended by hybrid nanoparticles over vertical cylinder by considering shape factor effect. J. Therm. Anal. Calorim. **25**, 1–5 (2020)
49. Ghadikolaei, S.S., Hosseinzadeh, K., Ganji, D.D.: Investigation on three dimensional squeezing flow of mixture base fluid (ethylene glycol-water) suspended by hybrid nanoparticle (Fe_3O_4–Ag) dependent on shape factor. J. Mol. Liq. **262**, 376–388 (2018)